



# Propofol Protects Regulatory T Cells, Suppresses Neurotoxic Astrogliosis, and Potentiates Neurological Recovery After Ischemic Stroke

Yuzhu Wang<sup>1,2</sup> · Dan Tian<sup>2</sup> · Yushang Zhao<sup>2</sup> · Mengyao Qu<sup>2</sup> · Yuhualei Pan<sup>2</sup> · Changwei Wei<sup>1</sup> · Yanbing Zhu<sup>2</sup> · Anshi Wu<sup>1</sup>

Received: 16 May 2020 / Accepted: 18 October 2020 / Published online: 20 March 2021  
© Center for Excellence in Brain Science and Intelligence Technology, CAS 2021

## Dear Editor,

Emergency intravascular thrombectomy is the best treatment for acute ischemic stroke [1]. However, it is controversial whether the use of general anesthesia during emergency intravascular thrombectomy affects patient recovery. The most commonly-used intravenous anesthetic for emergency surgery is propofol. Previous studies from our team as well as others found that propofol reduces infarct size and potentiates neurological recovery in the early phase of ischemic stroke in mice [2–4]. However, results from early time points do not fully reflect the influence of propofol on the dynamic progress of stroke. By tracking the RNA expression levels from 12 h to 21 days in a mouse stroke model, we established the first pseudotime paradigm of ischemic stroke, and demonstrated that regulatory T cells (Tregs) were the most important T cell component changed by propofol. We found that propofol altered the proportion of immune cells and changed the

levels of astrogliosis and neurogenesis in the later phase of ischemic stroke.

We simulated the rapid induction process of anesthesia for thrombectomy after acute ischemic stroke in the mouse model (Supplementary material; Materials and Methods). We administered propofol (16 mg/kg for mice) 1 min before reperfusion of the common carotid artery, and maintained propofol anesthesia for 2 h, to simulate the approximate duration of intravascular thrombectomy in our focal stroke mouse model.

To investigate the effects of propofol on stroke progression, we examined the neurological function of mice at 1, 3, 7, 14, and 21 days after reperfusion with propofol (stroke + propofol group) or normal saline (stroke group). In the contralateral sticky-tape test, mice in the stroke + propofol group needed less time to feel (latency) and tear off (removal time) the tape compared with the stroke group (Fig. 1A). In the contralateral whisker test, mice in the stroke + propofol group had a higher success ratio of same-side forelimb and cross-midline forelimb placing compared with the stroke group (Fig. 1B). The neurological results did not significantly differ between the stroke and stroke + propofol groups before stroke operation nor in the ipsilateral whisker test. These results indicate that propofol potentiates neurological recovery in mice with ischemic stroke.

To study the dynamic changes in the transcriptome after acute ischemic stroke, we performed RNA sequencing of the infarcted cortex at 12 h and 1, 3, 7, 14, and 21 days after stroke, and established a pseudotime paradigm for the mouse focal ischemic stroke model (stroke group). The unsupervised order of samples (in points) on the pseudotime trajectory was roughly consistent with the actual sampling time series (Fig. 1C), indicating that our pseudotime paradigm preserved the essential relationship

Yuzhu Wang and Dan Tian contributed equally to this work.

**Supplementary Information** The online version contains supplementary material available at <https://doi.org/10.1007/s12264-021-00653-4>.

✉ Yanbing Zhu  
zhuyanbing@ccmu.edu.cn

✉ Anshi Wu  
wuanshi88@163.com

<sup>1</sup> Department of Anesthesiology, Beijing Chaoyang Hospital, Capital Medical University, Beijing 100020, China

<sup>2</sup> Experimental and Translational Research Center, Beijing Friendship Hospital, Capital Medical University, Beijing 100050, China

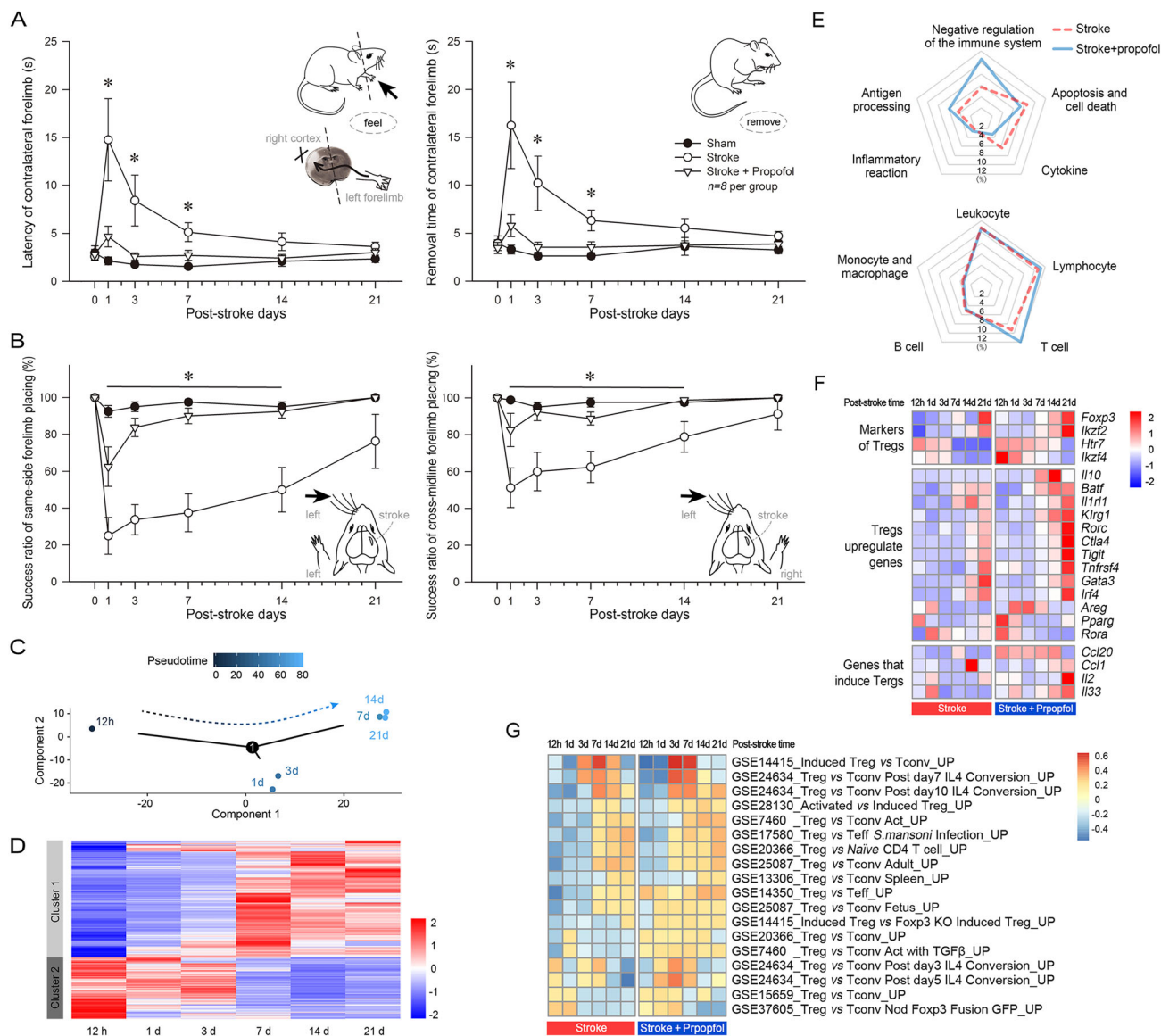


**Fig. 1.** Propofol-upregulated Tregs are the most important T cell component that change after ischemic stroke and they potentiate neurological recovery in mice. **A** Latency (left) and removal time (right) of contralateral sticky-tape test at the indicated time points after ischemic stroke onset. **B** Success ratio of contralateral whisker-evoked same-side (left) and cross-midline (right) forelimb placing test at the indicated time points after ischemic stroke onset. **C** Pseudotime trajectory of the minimum spanning tree of the focal ischemic stroke model. **D** Heatmaps of the relative expression levels of significant genes (rows) in pseudotime ordering along the actual sampling time (columns) after ischemic stroke. Cluster 1 (upper),  $n = 3,040$  genes;

between samples [5]. Next, we divided significantly changed genes [false discovery rate (FDR)  $< 0.05$  and  $P < 0.05$ ] in the pseudotime paradigm into two clusters. Genes in cluster 1 were up-regulated along pseudotime while genes in cluster 2 were down-regulated. Besides, when we returned to the real sampling time for verification, genes in cluster 1 had higher relative expression levels in

cluster 2 (lower),  $n = 1,645$  genes; significance level, FDR  $< 0.05$  and  $P < 0.05$ . **E** Radar plots of the top 5 bioprocesses (upper) and top 5 cell types (lower) identified by keyword frequency in significantly up-regulated biological process pathways from GO. **F** Heatmaps of characteristic genes of Tregs in the infarcted cortex at the indicated time points after stroke onset. **G** Relative enrichment scores of gene sets from different Treg-related databases at the indicated time points after stroke onset. GSE is the ID of databases from NCBI; Tregs, regulatory T cells; Tconvs, conventional T cells; Teffs, effector T cells; KO, knockout; GFP, green fluorescent protein. \* $P < 0.05$ , stroke + propofol group vs stroke group.

the real later phase of post-stroke time while genes in cluster 2 had lower relative expression levels (Fig. 1D).

Interestingly, in the enrichment analysis of up-regulated genes of cluster 1 (FDR  $< 0.05$  and adjusted  $P < 0.05$ ), all significant KEGG (Kyoto Encyclopedia of Genes and Genomes) pathways and 110 out of 140 significant GO (Gene Ontology) biological processes were involved in

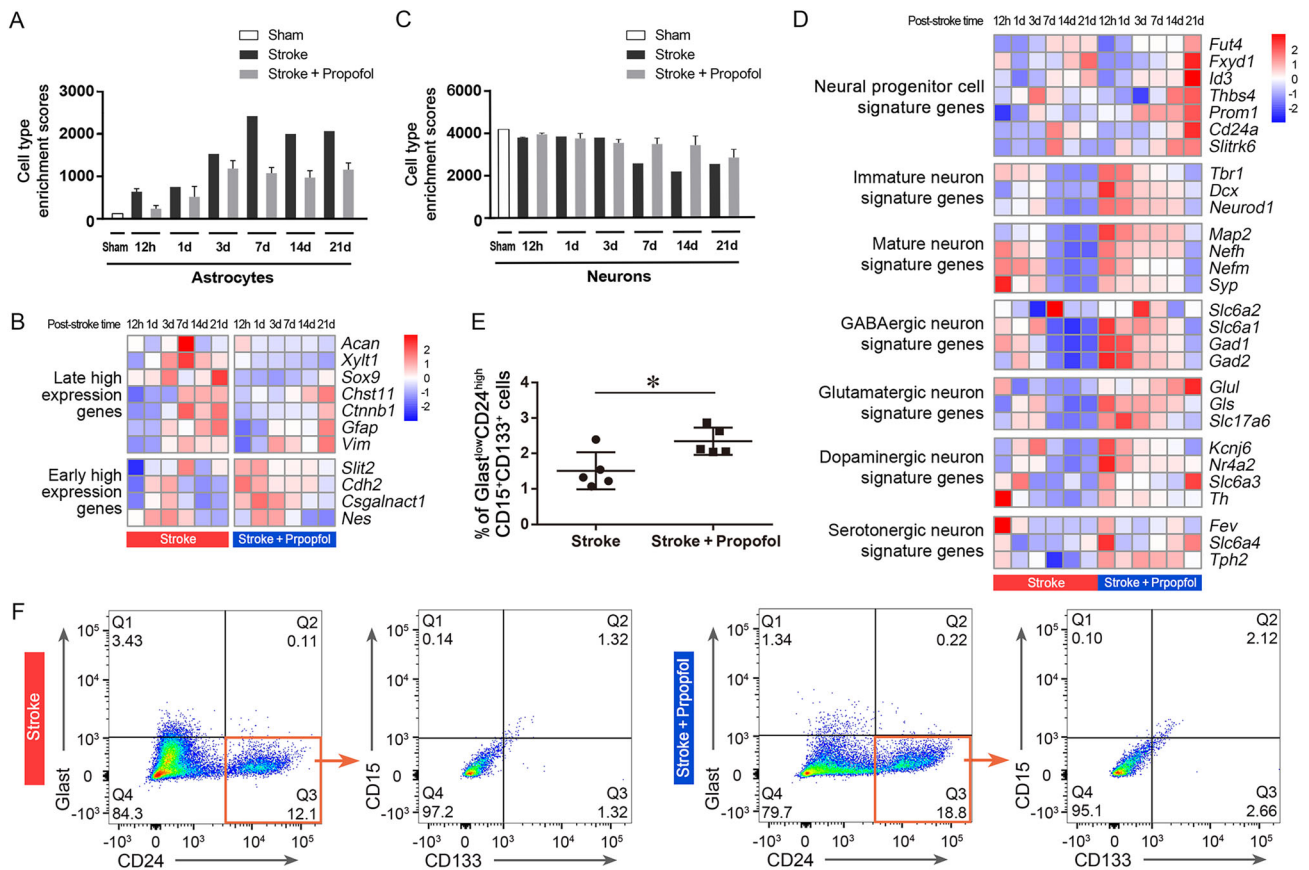


**Fig. 2.** Propofol inhibits neurotoxic astrogliosis and potentiates neurogenesis in mice after ischemic stroke. **A** Relative enrichment scores of astrocytes in the infarcted cortex at the indicated time points after stroke onset. **B** Heatmaps of relative expression levels of astrocyte signature genes in the infarcted cortex at the indicated time points after stroke onset. **C** Relative enrichment scores of neurons in the infarcted cortex at the indicated time points after stroke onset.

**D** Heatmaps of relative expression levels of signature genes of different kinds of neurons in the infarcted cortex at the indicated time points after stroke onset. **E, F** Statistical analysis and representative flow cytometry plots of Glast<sup>low</sup>CD15<sup>high</sup>CD133<sup>+</sup> cells from the infarcted cortex at 21 days after stroke ( $n = 5$ ,  $P = 0.021$ ,  $t$ -test). \* $P < 0.05$  in the stroke + propofol group vs stroke group.

immune responses (Fig. S1A, B). Genes in cluster 2 showed decreased neuronal function over pseudotime (Fig. S1E). Thus, immune responses dominated the major changes of acute ischemic stroke in the pseudotime paradigm.

Then, we performed RNA sequencing of the infarcted cortex at the same six time points and followed the same pseudotime paradigm in the stroke + propofol group. There were 2,686 genes significantly up-regulated along pseudotime and 1,355 down-regulated (FDR < 0.05 and  $P < 0.05$ ). Up-regulated biological processes and KEGG pathways in the stroke + propofol group also led to immune responses but differed in entries (Fig. S1C, D).

Next, we classified the significantly up-regulated biological processes of GO terms in the stroke and stroke + propofol groups using high-frequency words (Fig. 1E). Radar plots showed the distribution ratio of top keywords associated with bioprocesses (Fig. 1E upper) and keywords of cell types (Fig. 1E lower) of the two groups.

Interestingly, the proportions of negative regulation of immune responses and T cell-related biological processes of GO terms were higher in the propofol group than in the stroke group.

Since Tregs negatively regulate immune responses [5], we wondered whether these T cell-dominated as well as negatively regulated immune response changes in the stroke + propofol group were due to Tregs. Thus, we compared the expression levels of brain Treg-specific genes among groups [6]. Consistent with previous studies [6, 7], most Treg-specific genes had relatively low expression levels in the acute phase then gradually increased 14 days after ischemic stroke (Fig. 1F). Yet we found that *Htr7*, *Ikzf4*, *Areg*, *Pparg*, and *Rora* had relatively high levels in the early phase in our focal stroke model. As expected, propofol increased the expression levels of most Treg-specific genes with post-stroke time (Fig. 1F). Furthermore, we used 18 gene sets from 11 published Treg-related RNA-sequencing or microarray

data for verification [8]. Enrichment scores of gene sets that were up-regulated in Tregs were higher in the stroke + propofol group than at the corresponding time points of the stroke group (Fig. 1G).

Besides, inflammatory subtypes of T cells (CD4<sup>+</sup>, CD8<sup>+</sup>, and natural killer T cells) had lower enrichment scores in the stroke + propofol group than the stroke group at the corresponding time points (Fig. S1F), indicating that the increased T cell-related biological process terms in the stroke + propofol group were not due to inflammatory T cells. These results indicated that propofol promotes Tregs while inhibiting inflammatory T cells after stroke.

Given that Tregs suppress neurotoxic astrogliosis [6, 9], we analyzed the astrocyte enrichment signature in our ischemic stroke model, and found that propofol significantly attenuated the increase of astrocytes signature at each time point compared with the stroke group (Fig. 2A). In addition, astrocytes not only increased in population, but also changed in phenotype and biological function after central nervous system injury. Naïve astrocytes are activated after injury, then gradually switch to benign and tissue-repairing reactive astrocytes in the early phase, and later lapse into neurotoxic scar-forming astrocytes [10, 11]. In our stroke model, propofol increased the expression of reactive astrocyte-related genes and specifically inhibited scar-forming astrocyte-related genes during the recovery phase compared with the stroke group (Fig. 2B).

Along with the inhibition of neurotoxic astrogliosis, propofol maintained the enrichment score of neurons in the late phase of stroke (Fig. 2C), reducing the loss of neurons. The cortex in the stroke + propofol group had higher gene signature levels of different kinds of neurons than those in the stroke group (Fig. 2D). Moreover, neurotoxic astrocytes eventually become fibroblast astrocytes, further preventing neurogenesis and axon regeneration in the later stage of brain injury [10, 12]. We noted that the stroke + propofol group had higher gene expression levels of neural progenitor cells than those in the stroke group in the late phase (Fig. 2D). Flow cytometry confirmed that propofol increased the proportion of Glast<sup>low</sup>CD24<sup>high</sup>CD15<sup>+</sup>CD133<sup>+</sup> cells in the infarcted scar 21 days after stroke (Fig. 2E, F). These data indicated that propofol suppresses neurotoxic astrogliosis and protects neurogenesis in the late phase of ischemic stroke.

In conclusion, we established the first pseudotime paradigm of ischemic stroke in mice, and demonstrated that Tregs were the most important T cell component up-regulated by propofol. Propofol altered the distribution of immune cells, suppressing neurotoxic astrogliosis and potentiating neurogenesis in the late phase of ischemic

stroke (Fig. S1G). Our research provides reference for the selection of anesthesia methods during intravascular thrombectomy and suggests a potential protective effect of propofol on other perioperative ischemic and inflammatory diseases.

**Acknowledgements** This work was supported by the National Natural Science Foundation of China (81771139) and Beijing Natural Science Foundation (7194270).

**Conflict of interest** The authors declare no conflict of interest.

## References

1. Yang P, Zhang Y, Zhang L, Zhang Y, Treurniet KM, Chen W, *et al.* Endovascular thrombectomy with or without intravenous alteplase in acute stroke. *N Engl J Med* 2020, 382: 1981–1993.
2. Wang Y, Tian D, Wei C, Cui V, Wang H, Zhu Y, *et al.* Propofol attenuates  $\alpha$ -synuclein aggregation and neuronal damage in a mouse model of ischemic Stroke. *Neurosci Bull* 2020, 36: 289–298.
3. Gelb AW, Bayona NA, Wilson JX, Cechetto DF. Propofol anesthesia compared to awake reduces infarct size in rats. *Anesthesiology* 2002, 96: 1183–1190.
4. Wang W, Lu R, Feng DY, Liang LR, Liu B, Zhang H. Inhibition of microglial activation contributes to propofol-induced protection against post-cardiac arrest brain injury in rats. *J Neurochem* 2015, 134: 892–903.
5. Hyvärinen A, Oja E. Independent component analysis: algorithms and applications. *Neural Netw* 2000, 13: 411–430.
6. Ito M, Komai K, Mise-Omata S, Iizuka-Koga M, Noguchi Y, Kondo T, *et al.* Brain regulatory T cells suppress astrogliosis and potentiate neurological recovery. *Nature* 2019, 565: 246–250.
7. Stubbe T, Ebner F, Richter D, Engel O, Klehmet J, Roysl G, *et al.* Regulatory T cells accumulate and proliferate in the ischemic hemisphere for up to 30 days after MCAO. *J Cereb Blood Flow Metab* 2013, 33: 37–47.
8. Subramanian A, Tamayo P, Mootha VK, Mukherjee S, Ebert BL, Gillette MA, *et al.* Gene set enrichment analysis: a knowledge-based approach for interpreting genome-wide expression profiles. *Proc Natl Acad Sci U S A* 2005, 102: 15545–15550.
9. Liddelov SA, Guttenplan KA, Clarke LE, Bennett FC, Bohlen CJ, Schirmer L, *et al.* Neurotoxic reactive astrocytes are induced by activated microglia. *Nature* 2017, 541: 481–487.
10. Hara M, Kobayakawa K, Ohkawa Y, Kumamaru H, Yokota K, Saito T, *et al.* Interaction of reactive astrocytes with type I collagen induces astrocytic scar formation through the integrin-N-cadherin pathway after spinal cord injury. *Nat Med* 2017, 23: 818–828.
11. Okada S, Nakamura M, Katoh H, Miyao T, Shimazaki T, Ishii K, *et al.* Conditional ablation of Stat3 or Socs3 discloses a dual role for reactive astrocytes after spinal cord injury. *Nat Med* 2006, 12: 829–834.
12. Garber C, Vasek MJ, Vollmer LL, Sun T, Jiang X, Klein RS. Astrocytes decrease adult neurogenesis during virus-induced memory dysfunction via IL-1. *Nat Immunol* 2018, 19: 151–161.